

# MATHEMATICAL MODELLING OF CONTINUOUS ETHANOL FERMENTATION IN A MEMBRANE BIOREACTOR BY PERVAPORATION COMPARED TO CONVENTIONAL SYSTEM

KIRTHIGA MURALI\*, M. ABUKHALED\*\*, S. BALAMURUGAN\*, L. RAJENDRAN\*\*\*<sup>#</sup>

\*Department of Mathematics, Government Arts and Science College, Melur, India

\*\*Department of Mathematics and Statistics, American University of Sharjah, United Arab Emirates

\*\*\*Department of Mathematics, Academy of Maritime Education and Training (AMET), Deemed to be University, Chennai-603112, India 300041, <sup>#</sup>e-mail: raj\_sms@rediffmail.com

*Abstract.* Mathematical models of ethanol fermentation in continuous conventional bioreactor (CCBR) and continuous membrane bioreactor (CMBR) are discussed theoretically. Each of these models is a system of nonlinear equations containing nonlinear terms related to Monod model for each retention time at non-steady condition. Analytical expressions of cell growth, glucose consumption, and ethanol production are obtained using a new approach of the homotopy perturbation method. A detailed study of the parameters effects on each of the governing systems is also presented. The obtained analytical solution is shown to be in strong agreement with most reliable numerical methods.

*Key words:* Ethanol fermentation, membrane bioreactor, mathematical modelling, new homotopy perturbation method, nonlinear equations.

## INTRODUCTION

From greenhouse gas emission to continuous consumption of fossil fuels to increasing demand on global energy, the production of renewable energy such as biofuels has become a living necessity [7, 24]. It is believed that renewable energy can supply two-thirds of the total global energy demand and contribute to the bulk of the greenhouse gas emissions reduction by the year 2050 [16]. The productivity of the ethanol fermentation process, predominantly based on batch operation in the U.S. fuel ethanol industry, could be improved by the adoption of continues processing technology using microorganism [27]. In the processing of ethanol fermentation, microorganisms such as yeasts play an essential role. They are used in industrial plants due to valuable properties in ethanol yield, ethanol tolerance, ethanol productivity, growth in simple, inexpensive media and undiluted fermentation. As the main component in fermentation, yeasts affect the amount of

---

Received: December 2020;  
in final form January 2021.

ethanol yield [5]. Yeasts are unicellular (usually spherical) microorganisms of size 2–4  $\mu\text{m}$  and are present naturally in some products such as fruits, cereals and vegetables. Of the different species of fermentative microorganisms that have been identified, we mention *Saccharomyces cerevisiae*, *Kluyveromyces fragilis*, *Torulaspota* and *Zymomonas mobilis* [25]. In the production of ethanol by fermentation, the most commonly used microorganism is the *Saccharomyces cerevisiae* yeast for it is known to allow a better separation process after fermentation in addition to its production of lower toxin content [13].

An advantage of continuous fermentation processes is that it is likely to lead to a reduced process costs during ethanol production. The productivity of a fermentation system is the main measurement for evaluating the performance of a fermentation system. This productivity is the amount of produced product per unit of time and reactor volume. Several factors are known to influence the level of productivity such as the concentrations of substrates and cells, the specific product formation rate, and the dilution rate. Another advantage of a continuous process is higher volumetric productivity as compared to a repeated batch process. In addition, almost complete utilization of the substrate is desired to avoid unproductive loss of substrate [9, 10]. The continuous ethanol production with a membrane bioreactor at high acetic acid concentrations also discussed [31].

Developed in 1950s, pervaporation is a low-temperature, low-pressure unit operation and, because of the nature of the vapor-liquid equilibrium of ethanol-water, it has a built-in selectivity for ethanol at low concentrations. Pervaporation technology is now used commercially for solvent dehydration operations, water purification, and organic separation as a substitute for distillation [6]. Pervaporation operation can be accomplished with a commercially available membrane, where the specific objective is to achieve a stable, continuous fermentation by the recovery of an enriched ethanol stream from the fermentation broth by pervaporation with minimal loss of ethanol yield or cell productivity [9].

The main purpose of this paper is to derive approximate analytical expressions for biomass (cell growth), glucose consumption, and ethanol production for all possible values of parameters and to discuss the influence of kinetic parameters on concentrations.

## MATHEMATICAL FORMULATION OF THE PROBLEM

Generally, models of microbial kinetics for growth and fermentation processes can be described by nonlinear differential equations in which the change of fermented product rate, substrate consumption and biomass are related to ethanol ( $P$ ), glucose ( $S$ ) and biomass ( $X$ ) concentrations by the means of suitable functional representing some kinetic growth rate models [8]. Due to the concentration of the preventive substrate, the growth rate of the microorganism can be described by the Monod equation.

$$\mu = \frac{\mu_m \cdot S}{K_S + S} \quad (1)$$

where  $K_S$  [g L<sup>-1</sup>] is the substrate inhibition constant and  $\mu_m$  [h<sup>-1</sup>] is defined as the maximum specific cell growth rate. In the sense of Monod growth rate, the mathematical model for CMBR is represented by differential equations for the cell growth, substrate consumption, and ethanol production that are respectively [14]:

$$\frac{dX}{dt} = \frac{\mu_m \cdot S}{K_S + S} \cdot X + \frac{F_m - F_0}{V} \cdot X \quad (2)$$

$$\frac{dS}{dt} = \frac{F_0(S_0 - S) + F_m \cdot S}{V} + \frac{\mu_m \cdot S}{K_{SS} + S} \cdot \frac{X}{Y_{X/S}} \quad (3)$$

$$\frac{dP}{dt} = \frac{F_m(P - P_m) - F_0 \cdot P}{V} + \frac{\mu_m \cdot S}{K_{SP} + S} \cdot X \cdot Y_{P/X} \quad (4)$$

where  $F_m$ ,  $F_0$  and  $F$  represent permeate, input and output (overflow) volumetric flow rates [L h<sup>-1</sup>],  $V$  and  $t$  are the bioreactor working volume [L] and fermentation time [h] during each dilution rate.  $S_0$ ,  $S$  are substrate concentrations at input and output streams [g L<sup>-1</sup>],  $P_m$  and  $P$  are ethanol concentrations at permeate and output streams of bioreactor [g L<sup>-1</sup>]. Also,  $Y_{X/S}$  represents the yield of biomass concentration based on substrate utilization whereas  $Y_{P/S}$  represents yield of the product formation based on biomass concentration.

Substituting  $F_m = 0$  in the above equations produces the corresponding continuous conventional bioreactor (CCBR), which is represented by differential equations for the cell growth, substrate consumption, and ethanol production that are, respectively, given by:

$$\frac{dX}{dt} = \frac{\mu_m \cdot S}{K_{SX} + S} \cdot X - \frac{F_0}{V} \cdot X \quad (5)$$

$$\frac{dS}{dt} = \frac{F_0(S_0 - S)}{V} + \frac{\mu_m \cdot S}{K_{SS} + S} \cdot \frac{X}{Y_{X/S}} \quad (6)$$

$$\frac{dP}{dt} = \frac{\mu_m \cdot S}{K_{SP} + S} \cdot X \cdot Y_{P/X} - \frac{F_0 \cdot P}{V} \quad (7)$$

The boundary conditions for the systems (2)–(4) and (5)–(7) are:

$$X(t=0) = X_i, S(t=0) = S_i, P(t=0) = P_i \quad (8)$$

Recently genetic algorithm used to determine kinetic model parameters [14]. A genetic algorithm is an optimization technique that is widely used to solve

chemical engineering problems [30]. Also, nonlinear least-squares method used to determine kinetic parameters of ethanol production from sweet sorghum juice [4]. Other reliable numerical approaches that can be used to obtain highly accurate numerical solution for the CMBR and CCBR models include wavelets [1], finite element method [12], and spline collocations [20].

However, obtaining analytical or semi-analytical solutions for nonlinear models is much more desired than numerical solutions for that analytical solution gives better insights on kinetic parameters or how a governing equation is sensitive to these parameters. Analytical solutions can be obtained by various methods such as variational iteration method [2, 19], differential transformation method [11] Green's function method [3, 21].

### A MODIFIED FORM OF THE HOMOTOPY PERTURBATION METHOD (MFHPM)

One of the widely used methods for solving nonlinear equations is the homotopy perturbation method (HPM). It was First introduced in 1999 [17]. HPM has been employed by many researchers to obtain approximate analytical solutions for nonlinear engineering dynamical systems [15, 18, 23, 26, 28]. Many researchers have modified HPM to achieve higher accuracy and faster convergence [22, 29].

#### ANALYTICAL EXPRESSION FOR CONCENTRATION OF BIOMASS, SUBSTRATE AND PRODUCT USING MEHPM

We construct the homotopy for the CMPR model given in Eq. (2) as follows:

$$(1-p) \cdot \left\{ \frac{dX}{dt} - X \cdot \left[ \frac{\mu_m}{(K_{SX}/S(t=0)) + 1} + \frac{F_m - F_0}{V} \right] \right\} + p \cdot \left\{ \frac{dX}{dt} - \frac{\mu_m S}{K_{SX} + S} \cdot X - \frac{F_m - F_0}{V} \right\} = 0 \quad (9)$$

The approximate solution of Eq. (9) is expressed in the series form:

$$X = p^0 \cdot X_{\text{zeroth}} + p^1 \cdot X_{\text{first}} + p^2 \cdot X_{\text{second}} + \dots \quad (10)$$

Substituting Eq. (10) into Eq. (9) and equate like powers of  $p$  gives a system of equations. For example, the equation derived from the powers of  $p^0$  is:

$$\frac{dX_{\text{zeroth}}}{dt} - X_{\text{zeroth}} \cdot \left[ \frac{\mu_m \cdot S}{(K_{SX}/S_i) + 1} + \frac{F_m - F_0}{V} \right] = 0 \quad (11)$$

subject to the initial conditions:

$$\text{at } t = 0, X_{\text{zeroth}}(0) = X_i, S_{\text{zeroth}}(0) = S_i \quad (12)$$

Solving Eqs. (11)–(12), gives  $X_{\text{zeroth}}$  as follows:

$$X_{\text{zeroth}} = X_i \cdot e^{-\alpha t} \quad (13)$$

where:

$$\alpha = \frac{F_0 - F_m}{V} - \frac{\mu_m}{(K_{SX/S_i} + 1)} \quad (14)$$

By substituting Eq. (13) into Eq. (10) and assuming that  $X(t) \cong X_{\text{zeroth}}(t)$  gives one term analytical approximation of the cell growth. Likewise, we obtain the following one term analytical expressions for the substrate consumption and ethanol production for the CMBR model given in Eqs. (3)–(4):

$$S(t) = e^{\lambda t} \cdot \left( S_i - \frac{\alpha \cdot \beta}{\lambda(\lambda - \alpha)} + \frac{\beta + \gamma}{\lambda - \alpha} \right) - \frac{\beta + \gamma \cdot e^{\alpha t}}{\lambda - \alpha} + \frac{\alpha \cdot \beta}{\lambda(\lambda - \alpha)} \quad (15)$$

$$P(t) = e^{\lambda t} \cdot \left( P_i - \frac{\kappa}{\alpha - \lambda} + \frac{\sigma}{\lambda} \right) + \frac{\kappa}{\alpha - \lambda} \cdot e^{\lambda t} + \frac{\alpha}{\lambda} \quad (16)$$

where:

$$\beta = \frac{F_0 \cdot S_0}{V}, \lambda = \frac{F_m \cdot F_0}{V}, \gamma = \frac{\mu_m \cdot X_i}{((K_{SX/S_i} + 1) \cdot Y_{X/S})}, \sigma = \frac{F_m \cdot P_m}{V}, \kappa = \frac{\mu_m \cdot Y_{X/P} \cdot X_i}{(K_{SX/S_i} + 1)} \quad (17)$$

In the same fashion, the MFHPM is applied to obtain the following analytical expressions of the cell growth, substrate consumption, and ethanol production for the CCBR given in Eqs. (5)–(7):

$$X(t) = X_i \cdot e^{-\alpha_1 t} \quad (18)$$

$$S(t) = e^{\alpha_1 t} \cdot \left( S_i - \frac{\gamma}{\alpha_1 + \lambda_1} - \frac{\beta}{\lambda_1} \right) + \frac{\gamma \cdot e^{-\alpha_1 t}}{\alpha_1 + \lambda_1} + \frac{\beta}{\lambda_1} \quad (19)$$

$$P(t) = e^{\lambda_1 t} \cdot \left( P_i - \frac{\kappa}{\alpha_1 - \lambda_1} - \frac{\beta}{\lambda_1} \right) + \frac{\kappa \cdot e^{\alpha_1 t}}{\alpha_1 - \lambda_1} \quad (20)$$

where:

$$\alpha_1 = \frac{F_0}{V} - \frac{\mu_m}{((K_{SX/S_i} + 1))}, \lambda_1 = \frac{F_0}{V} \quad (21)$$

The dilution rate ( $h^{-1}$ ), can be computed from the formula:

$$d = \frac{\text{volumetric flowrate}}{\text{bioreactor working volume}} = \frac{F_m - F_0}{V} \quad (22)$$

### NUMERICAL SIMULATION

To investigate the accuracy of the analytical solution with a finite number of terms, the systems of differential equations represented by Eqs. (2)–(4) for the CMBR model and Eqs. (5)–(7) for the CCBR model are solved numerically with the powerful Runge-Kutta method using the MATLAB function ode45. The obtained analytical expressions of cell growth, ethanol production, and glucose concentration, which are obtained based on Monod kinetic models during each retention time at non-steady conditions, show strong agreement with numerical solutions as shown in Figures 1–7. Tables 3–6 confirm that the averages of variations between the analytical solutions and the numerical results for biomass and glucose concentrations for both CMBR-Monod and CCBR-Monod for various values are very small.

### RESULTS AND DISCUSSION

Analytical expressions of cell, glucose and ethanol concentrations during the fermentation at different retention times are derived in Eqs. (13) – (16) and Eqs. (18) – (20) under both membrane and conventional bioreactors, respectively.

Figure 1 describes the cell growth, substrate concentration and ethanol production during continuous membrane and continuous conventional bioreactor at different retention times under non-steady state condition. It is noticed from Figure 1 that cell growth and ethanol production drastically decrease at the rising fermentation time while glucose consumption increases.

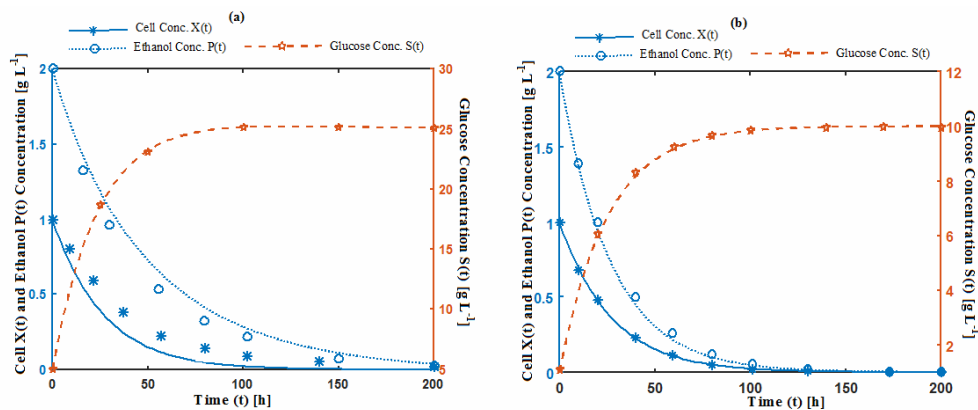


Fig. 1. Concentration profiles of cell growth, glucose consumption and ethanol production. Figure (a) is for the CMBR Monod and Figure (b) is for the CCBR Monod.

The cell concentration profiles for the CMBR case are illustrated in Figure 2. It is observed from Figure 2(a) that cell concentration increases as bioreactor working volume  $V$  increases and reaches a steady state. Also, from Figures 2(b) and 2(c), it is inferred that no significant changes occur in concentration of cell growth with respect to maximum specific cell growth rate  $\mu_m$  or substrate inhibition constant  $K_{SX}$ . However, Figure 2(d) points out that as input and permeate volumetric flow rates,  $F_0$  and  $F_m$  decrease, the cell concentration increases.

Glucose concentration profiles under CMBR for various parameters are illustrated in Figure 3. It is concluded from Figure 3(a) that glucose concentration is inversely proportional to volume where the fermentation process goes exponentially and reaches a steady state. Figures 3(b) and 3(c) show that glucose concentration is independent of maximum specific cell growth rate, yield coefficient, substrate inhibition, or glucose consumption changes. Figure 3(d) states that the permeate volumetric flow rates increases, glucose concentration decreases and reaches stationary phase where the fermentation process stops growing. But a decrease in the substrate concentration at the input stream leads to a reduction in glucose consumption as confirmed by Figure 3(e).

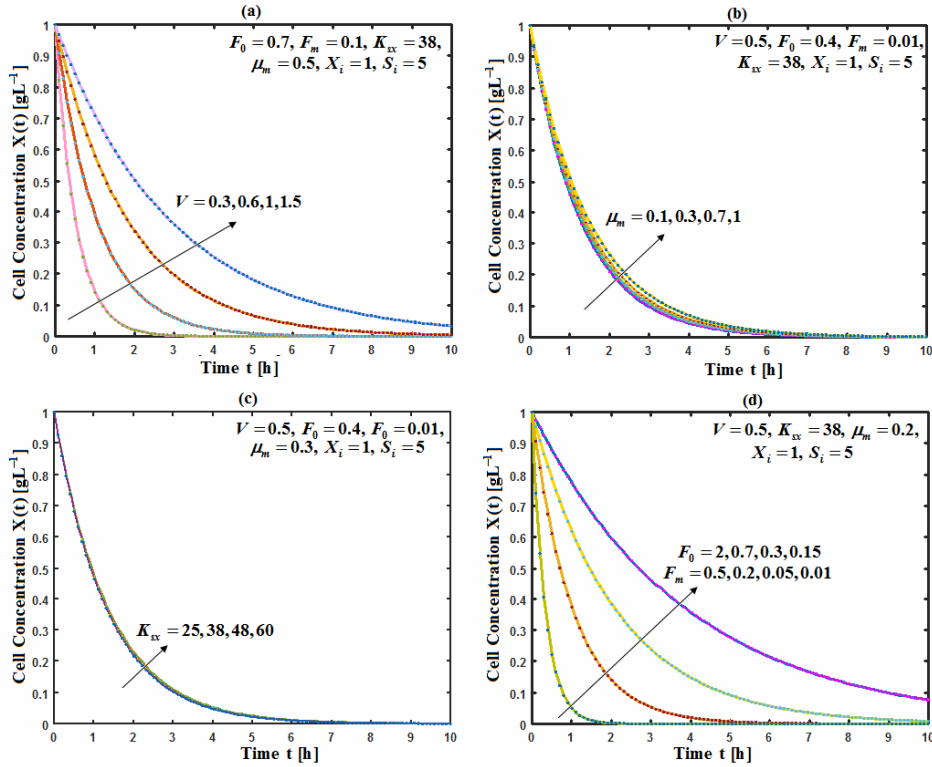


Fig. 2. Concentration profile of cell growth *versus* time for the CMBR Monod. Solid line represents analytical solution (Eq. (13)) while dotted line is the numerical result.

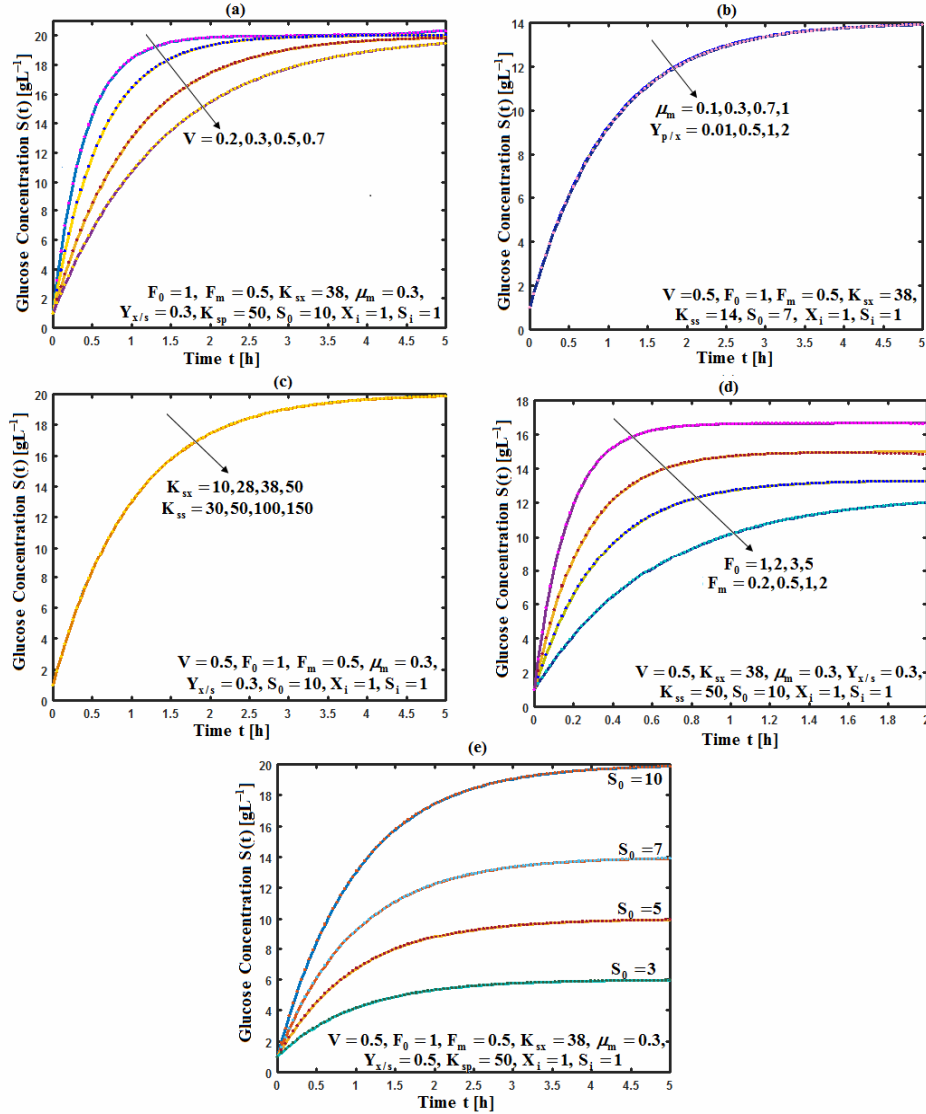


Fig. 3. Concentration profile of glucose *versus* time for the CMBR Monod. Solid line is the analytical solution given in Eq. (15) and dotted line is the numerical result.

The complex effects of the various kinetic parameters on ethanol concentration in CMBR are depicted in Figure 4. It is noticed in Figure 4(a) that ethanol concentration decreases when volume increases. Figure 4(b), however, shows no significant change in ethanol concentration takes place when the values of maximum specific cell growth rate or product yield coefficient change. Likewise, no changes in ethanol concentration are noticed if substrate inhibition

constants for glucose consumption and ethanol production changes (Fig. 4(c)) nor will be any changes if ethanol concentration at permeate of bioreactor changes (Fig. 4(e)). Also, ethanol production is inversely proportional to volumetric flow rates. Figure 4(d) clearly points out that the input and permeate volumetric flow rates,  $F_0$  and  $F_m$ , decrease while ethanol concentration increases.

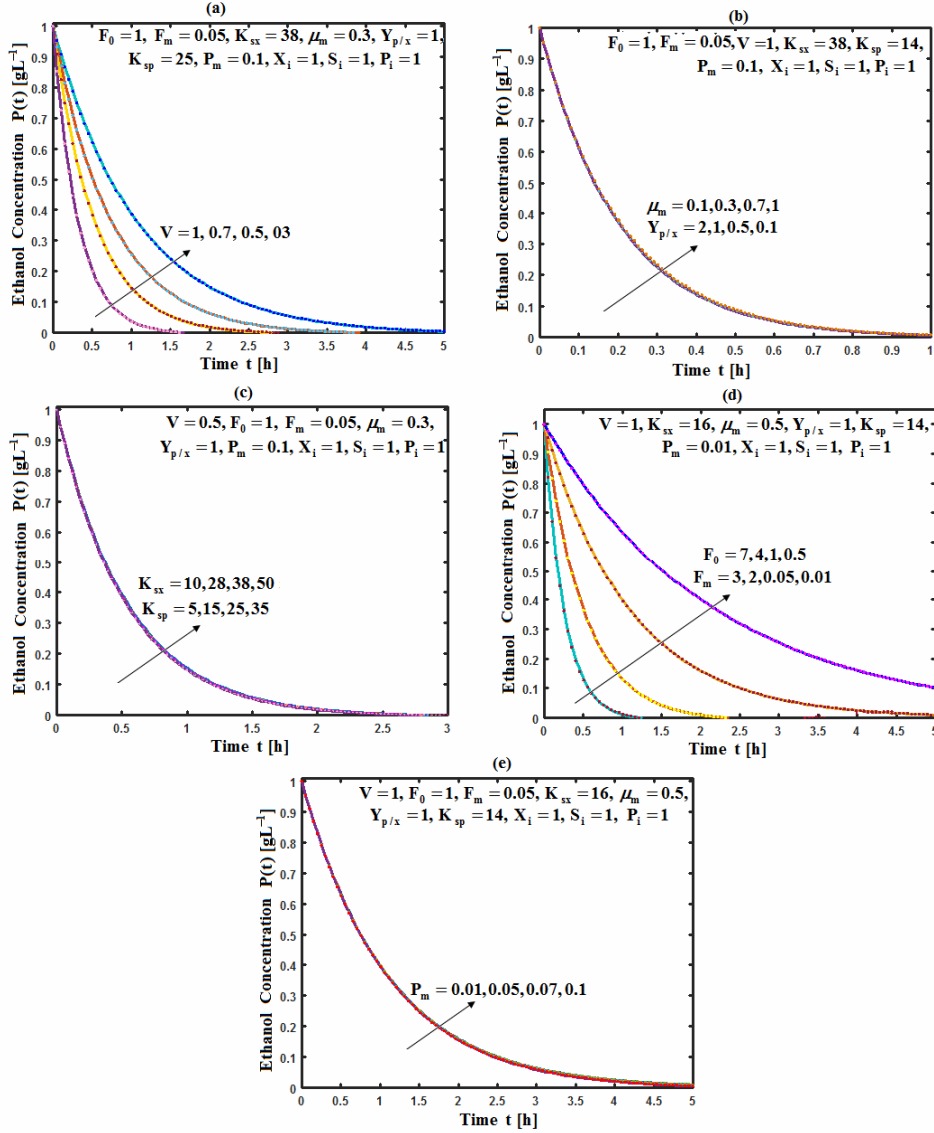


Fig. 4. Profile of concentration of ethanol *versus* time for the CMBR Monod. Solid line is an analytical solution from Eq. (16) and the dotted line is the numerical result.

The behavior of cell concentration under CCBR is similar to that under CMBR as shown in Figure 5. The cell concentration increases as bioreactor working volume  $V$  increases and reaches steady state (Fig. 5(a)). Also, from Figures 5(b) and 5(c), we notice that there are no significant changes occur in cell concentration for varying the maximum specific cell growth rate  $\mu_m$  or substrate inhibition constant for cell growth,  $K_{sx}$ . Also, cell concentration increases when input and permeate volumetric flow rates,  $F_0$  and  $F_m$ , decrease (Fig. 5(d)).

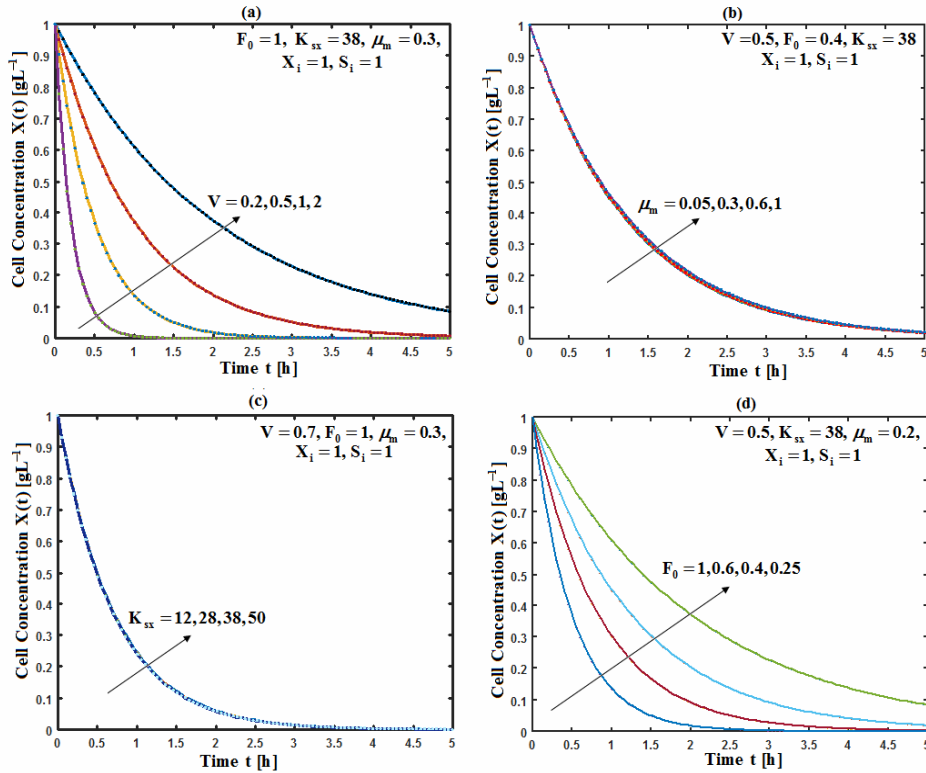


Fig. 5. Profile of concentration of cell growth *versus* time for CCBR Monod. Solid line is the analytical solution from Eq. (18) and dotted line is the numerical result.

Glucose concentration behavior under CCBR is similar to that under CMBR. From Figure 6(a), it is noticed that glucose concentration is inversely proportional to volume. Also, no significant changes in glucose concentration about the parameters such as maximum specific growth rate, yield coefficient, substrate inhibition constant ((Figs 6(b), and 6(c)). But the increase of input and volumetric flow rates lead to decreases in glucose concentration (Fig. 6(d)).

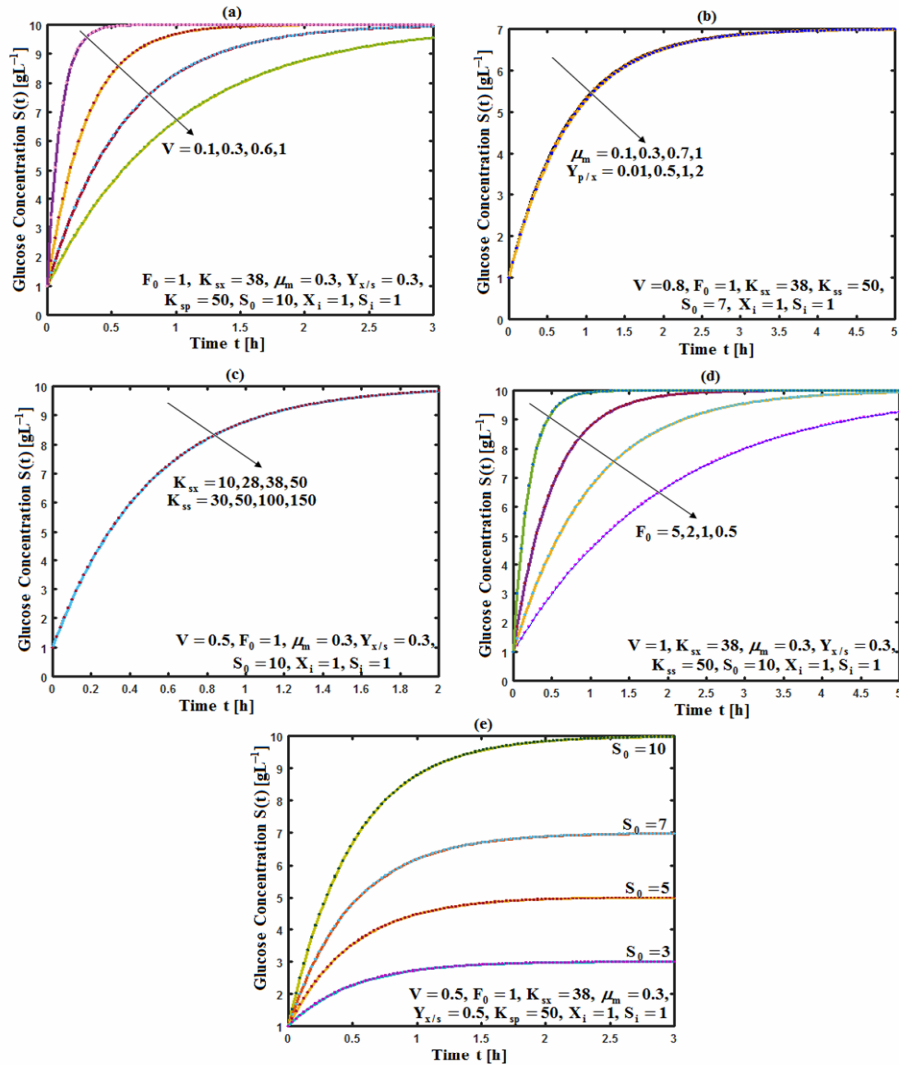


Fig. 6. Profile of concentration of glucose *versus* time for the CCBR Monod. Solid line is the analytical solution from Eq. (19) and dotted line is the numerical result.

The complex effects of the various kinetic parameters on ethanol concentration in CCBR are shown in Figure 7. It is shown in Figure 7(a) that ethanol concentration decreases when volume increases for decreasing time. But Figure 7(b) shows that the concentration does not show significant changes as the values of maximum specific cell growth rate or product yield coefficient change. Substantial changes take place in concentration as the values for the substrate inhibition constants for glucose consumption or product production change (Fig. 7(c)). In Figure 7(d), it is noted that ethanol production is directly proportional to input volumetric flow rates.

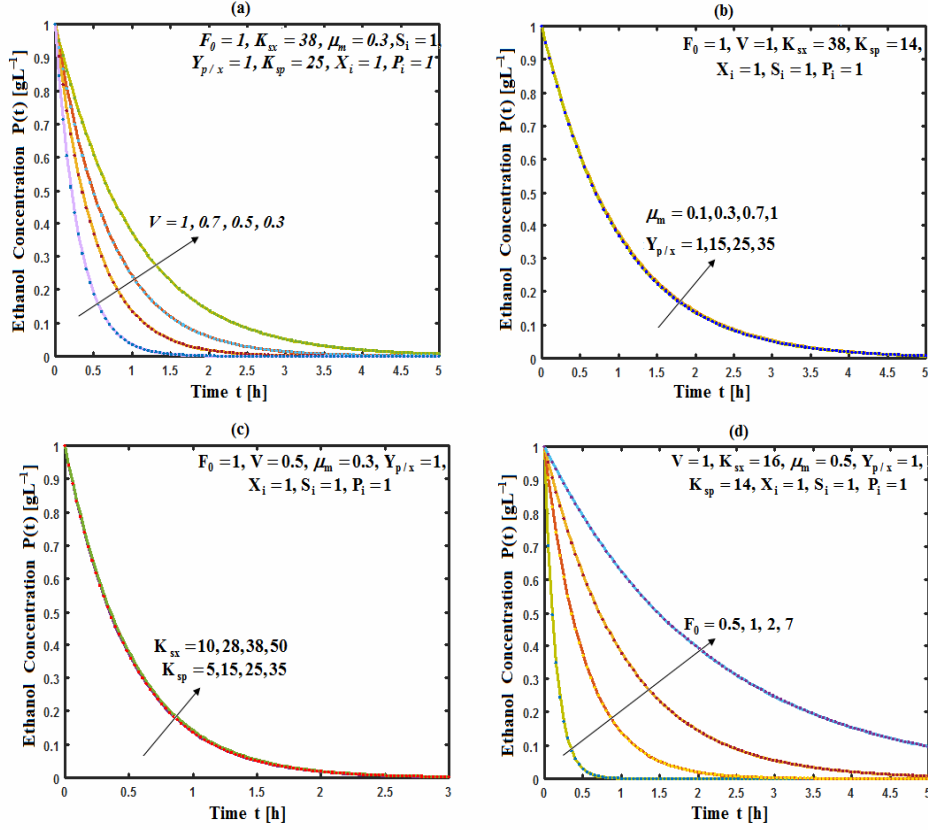


Fig. 7. Profile of concentration of glucose *versus* time: Solid line is an analytical solution from Eq. (23) and the dotted line is the numerical results.

Figures 8(a) and 8(b) show high cell concentration and glucose consumption in CMBR for each fermentation time over the dilution rate. It is noted from Figure 8(a) that due to the cell washout and lack of adequate time, the cell concentration decreases with the increase of dilution rate. Also, less substrate inhibition antecedent to further cell growth with lower time and dilution rate (Fig. 8(b)). The ethanol productivity over time and dilution rate is presented in Figure 8(c), where it is concluded that up to the dilution rate, the ethanol production raised and then declined because of cell washout with sufficient time. Thus, the maximum productivity did not occur at the maximum conversion of substrate.

The maximum and minimum values of cell growth, glucose, and ethanol production in terms of kinetic parameters on CMBR and CCBR are summarized in Tables 1 and 2.

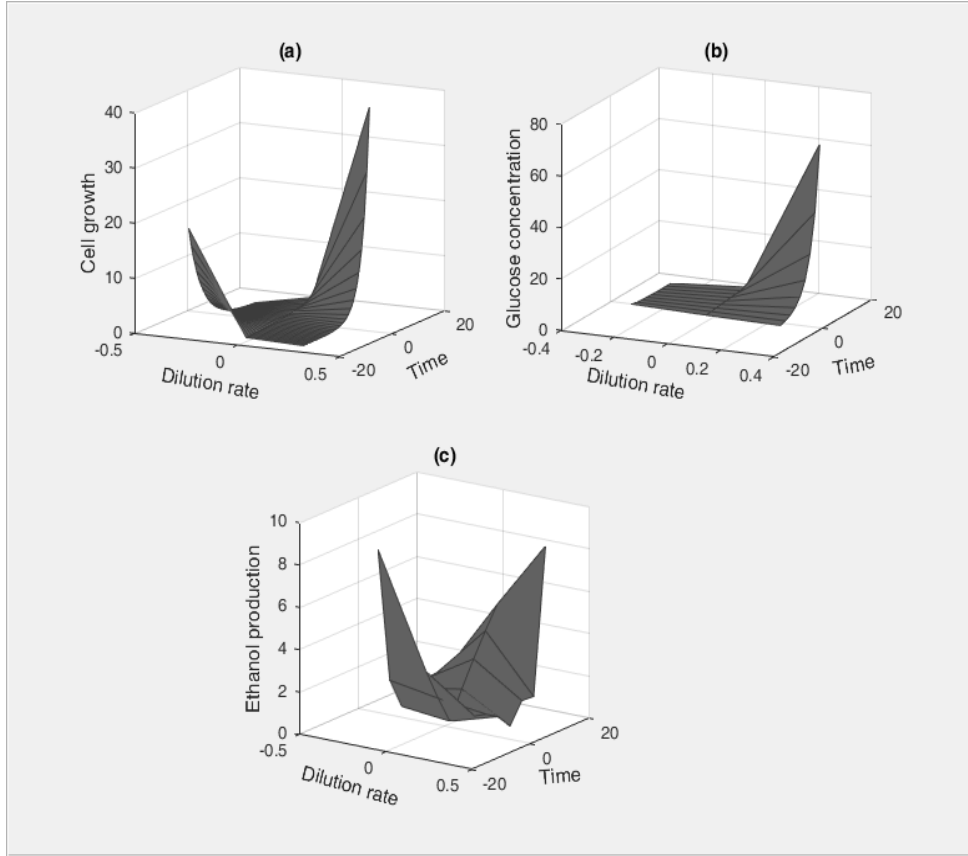


Fig. 8. Plot of cell growth ( $\text{g L}^{-1}$ ) (a), glucose concentration ( $\text{g L}^{-1}$ ) (b), ethanol production ( $\text{g L}^{-1}$ ) (c), versus time (h) and dilution rate ( $\text{h}^{-1}$ ) (Eq. (22)).

Table 1

The maximum and minimum values of the biomass formation, substrate utilization, and ethanol production in terms of kinetic parameters for CMBR-Monod are summarized

| Product                | Maximum   | Minimum                                   |
|------------------------|---|---|
| Biomass                | $X = 0$   | $X = X_i$ (initial biomass concentration) |
| Glucose<br>(Substrate) | $S = \frac{\beta}{\lambda - \alpha} + \frac{\alpha \cdot \beta}{\lambda(\lambda - \alpha)}$ | $S = S_i$ (initial glucose concentration) |
| Ethanol<br>(Product)   | $P = \frac{\alpha}{\lambda}$  | $P = P_i$ (initial ethanol concentration) |

Table 2

The maximum and minimum values of the biomass formation, substrate utilization and ethanol production in terms of kinetic parameters for CCBR-Monod are summarized

| Product                | Maximum                       | Minimum                                   |
|------------------------|-------------------------------|---|
| Biomass                | $X = 0$                       | $X = X_i$ (initial biomass concentration) |
| Glucose<br>(Substrate) | $S = \frac{\beta}{\lambda_1}$ | $S = S_i$ (initial glucose concentration) |
| Ethanol<br>(Product)   | $P = 0$                       | $P = P_i$ (initial ethanol concentration) |

Table 3

Comparison of biomass concentration (Eq. (13)) with numerical simulation for values of  $X(t)$  and other experimental values of parameters for CMBR-Monod

| $X(t)$ biomass concentration ( $\text{g L}^{-1}$ ) |                     |          |                   |                     |          |                   |
|--|---------------------|----------|-------------------|---------------------|----------|-------------------|
| $t$ (h)  | $V = 0.3 \text{ L}$ |          |                   | $V = 0.6 \text{ L}$ |          |                   |
|  | Numerical           | Eq. (13) | % error deviation | Numerical           | Eq. (13) | % error deviation |
| 0  | 1.0000              | 1.0000   | 0.0000            | 1.0000              | 1.0000   | 0.0000            |
| 2  | 0.0200              | 0.0205   | 0.0244            | 0.1459              | 0.1520   | 0.0419            |
| 4  | 0.0003              | 0.0004   | 0.3333            | 0.0220              | 0.0231   | 0.0495            |
| 6  | 0.0000              | 0.0000   | 0.0000            | 0.0035              | 0.0035   | 0.0112            |
| 8  | 0.0000              | 0.0000   | 0.0000            | 0.0005              | 0.0005   | 0.0000            |
| 10   | 0.0000              | 0.0000   | 0.0000            | 0.0000              | 0.0000   | 0.0000            |
|  | Average error %     |          | 0.0596            | Average error %     |          | 0.0171            |
|  | $V = 1 \text{ L}$   |          |                   | $V = 1.5 \text{ L}$ |          |                   |
|  | Numerical           | Eq. (13) | % error deviation | Numerical           | Eq. (13) | % error deviation |
| 0  | 1.0000              | 1.0000   | 0.0000            | 1.0000              | 1.0000   | 0.0000            |
| 2  | 0.3269              | 0.3383   | 0.0349            | 0.4962              | 0.5047   | 0.0171            |
| 4  | 0.1136              | 0.1144   | 0.0076            | 0.258               | 0.2547   | 0.0127            |
| 6  | 0.0367              | 0.0387   | 0.0541            | 0.1272              | 0.1285   | 0.0102            |
| 8  | 0.0125              | 0.0131   | 0.0482            | 0.0644              | 0.0649   | 0.0074            |
| 10   | 0.0044              | 0.0044   | 0.0006            | 0.0327              | 0.0327   | 0.0018            |
|  | Average error %     |          | 0.0241            | Average error %     |          | 0.0082            |

Table 4

Comparison of glucose concentration (Eq. (15)) with numerical simulation for values of  $S(t)$  and other experimental values of parameters for CMBR-Monod

| $S(t)$ glucose concentration ( $\text{g L}^{-1}$ ) |                 |          |                   |                 |          |                   |
|--|-----------------|----------|-------------------|-----------------|----------|-------------------|
| $t$ (h)  | $V = 0.2$ L     |          |                   | $V = 0.3$ L     |          |                   |
|  | Numerical       | Eq. (15) | % error deviation | Numerical       | Eq. (15) | % error deviation |
| 0  | 1.0000          | 1.0000   | 0.0000            | 1.0000          | 1.0000   | 0.0000            |
| 1  | 18.4500         | 18.4419  | 0.0004            | 16.4100         | 16.4150  | 0.0003            |
| 2  | 19.8800         | 19.8722  | 0.0003            | 19.3200         | 19.3236  | 0.0001            |
| 3  | 19.9000         | 19.9895  | 0.0045            | 19.8700         | 19.8723  | 0.0001            |
| 4  | 20.0000         | 19.9991  | 0.0004            | 19.9700         | 19.9759  | 0.0003            |
| 5  | 20.0000         | 19.9999  | 0.0000            | 20.0000         | 19.9954  | 0.0002            |
|  | Average error % |          | 0.0009            | Average error % |          | 0.0001            |
| $t$ (h)  | $V = 0.5$ L     |          |                   | $V = 0.7$ L     |          |                   |
|  | Numerical       | Eq. (15) | % error deviation | Numerical       | Eq. (15) | % error deviation |
| 0  | 1.0000          | 1.0000   | 0.0000            | 1.0000          | 1.0000   | 0.0000            |
| 1  | 13.1100         | 13.0175  | 0.0070            | 10.6000         | 10.7083  | 0.0102            |
| 2  | 17.4300         | 17.4339  | 0.0002            | 15.3900         | 15.4561  | 0.0042            |
| 3  | 19.0500         | 19.0570  | 0.0003            | 17.7700         | 17.7779  | 0.0004            |
| 4  | 19.6500         | 19.6534  | 0.0001            | 18.9600         | 18.9133  | 0.0024            |
| 5  | 19.8700         | 19.8726  | 0.0001            | 19.4700         | 19.4686  | 0.0000            |
|  | Average error % |          | 0.0012            | Average error % |          | 0.0028            |

Table 5

Comparison of biomass concentration (Eq. (18)) with numerical simulation for values of  $X(t)$  and other experimental values of parameters for CCBR-Monod

| $X(t)$ biomass concentration ( $\text{g L}^{-1}$ ) |             |          |                   |             |          |                   |
|--|-------------|----------|-------------------|-------------|----------|-------------------|
| $t$ (h)  | $V = 0.2$ L |          |                   | $V = 0.5$ L |          |                   |
|  | Numerical   | Eq. (18) | % error deviation | Numerical   | Eq. (18) | % error deviation |
| 0  | 1.0000      | 1.0000   | 0.0000            | 1.0000      | 1.0000   | 0.0000            |
| 1  | 0.0065      | 0.0067   | 0.0435            | 0.1342      | 0.1363   | 0.0162            |
| 2  | 0.0000      | 0.0000   | 0.0000            | 0.0177      | 0.0185   | 0.0485            |
| 3  | 0.0000      | 0.0000   | 0.0000            | 0.0026      | 0.0025   | 0.0353            |

|   |                 |          |                   |                 |          |                   |
|---|-----------------|----------|-------------------|-----------------|----------|-------------------|
| 4 | 0.0000          | 0.0000   | 0.0000            | 0.0003          | 0.0003   | 0.0000            |
| 5 | 0.0000          | 0.0000   | 0.0000            | 0.0000          | 0.0000   | 0.0000            |
|   | Average error % |          | 0.00725           | Average error % |          | 0.0166            |
|   | V = 1 L         |          |                   | V = 2 L         |          |                   |
|   | Numerical       | Eq. (18) | % error deviation | Numerical       | Eq. (18) | % error deviation |
| 0 | 1.0000          | 1.0000   | 0.0000            | 1.0000          | 1.0000   | 0.0000            |
| 1 | 0.3739          | 0.3707   | 0.0085            | 0.6018          | 0.6112   | 0.0156            |
| 2 | 0.1357          | 0.1374   | 0.0127            | 0.3583          | 0.3735   | 0.0426            |
| 3 | 0.0498          | 0.0509   | 0.0204            | 0.2221          | 0.2283   | 0.0280            |
| 4 | 0.0180          | 0.0188   | 0.0438            | 0.1357          | 0.1395   | 0.0284            |
| 5 | 0.0070          | 0.0070   | 0.0000            | 0.0853          | 0.0853   | 0.0000            |
|   | Average error % |          | 0.0142            | Average error % |          | 0.0191            |

Table 6

Comparison of glucose concentration (Eq. (19)) with numerical simulation for values of  $S(t)$  and other experimental values of parameters for CCBR-Monod

| $S(t)$ glucose concentration ( $\text{g L}^{-1}$ ) |                 |          |                   |                 |          |                   |
|--|-----------------|----------|-------------------|-----------------|----------|-------------------|
| $t$ (h)  | V = 0.1 L       |          |                   | V = 0.3 L       |          |                   |
|  | Numerical       | Eq. (19) | % error deviation | Numerical       | Eq. (19) | % error deviation |
| 0  | 1.0000          | 1.0000   | 0.0000            | 1.0000          | 1.0000   | 0.0000            |
| 1  | 10.0000         | 9.9995   | 0.0000            | 9.6960          | 9.6796   | 0.0016            |
| 2  | 10.0000         | 9.9999   | 0.0000            | 9.9890          | 9.9885   | 0.0000            |
| 3  | 10.0000         | 9.9999   | 0.0000            | 10.0000         | 9.9995   | 0.0000            |
|  | Average error % |          | 0.0000            | Average error % |          | 0.0004            |
|  | V = 0.6 L       |          |                   | V = 1 L         |          |                   |
|  | Numerical       | Eq. (19) | % error deviation | Numerical       | Eq. (19) | % error deviation |
| 0  | 1.0000          | 1.0000   | 0.0000            | 1.0000          | 1.0000   | 0.0000            |
| 1  | 8.3370          | 8.3038   | 0.0039            | 6.5860          | 6.6963   | 0.0167            |
| 2  | 9.6680          | 9.6803   | 0.0012            | 8.7300          | 8.7873   | 0.0065            |
| 3  | 9.9400          | 9.9397   | 0.0000            | 9.5550          | 9.5548   | 0.0000            |
|  | Average error % |          | 0.0012            | Average error % |          | 0.0058            |

## CONCLUSIONS

A theoretical one-dimensional model of ethanol fermentation in a CCBP and a CMBP are discussed. The time-independent nonlinear ordinary differential equations of concentration of cell growth (biomass), substrate and ethanol have been solved analytically using a modified homotopy perturbation method. The effect of kinetic parameters such as Maximum specific cell growth rate ( $\mu_m$ ), Substrate inhibition constant for biomass, substrate, product ( $K_{SX}$ ,  $K_{SS}$ ,  $K_{SP}$ ), Input and permeate volumetric flow rates ( $F_0$ ,  $F_m$ ), Ethanol concentration at permeate of bioreactor ( $P_m$ ), yield coefficients for biomass and product ( $Y_{XS}$ ,  $Y_{PX}$ ), Bioreactor working volume ( $V$ ) on concentration of cell growth, substrate (glucose) and product (ethanol) are discussed. The proposed analytical model was in satisfactory agreement when it was successfully compared to numerical ones with experimental data. The theoretical results demonstrated that in order to achieve low substrate consumption and ethanol production.

## Appendix A (Notations)

| Symbol   | Description   | Values  | Symbol  | Description   | Values |
|----------|---|---------|---|---|--------|
| $X(t)$   | Concentration of biomass ( $\text{g L}^{-1}$ )                              |         | $F_0$   | Input volumetric flow rates ( $\text{L h}^{-1}$ )                                   | 6      |
| $S(t)$   | Concentration of substrate (glucose) ( $\text{g L}^{-1}$ )                  |         | $F_m$   | Permeate volumetric flow rates ( $\text{L h}^{-1}$ )                                | 10     |
| $P(t)$   | Concentration of product (ethanol) ( $\text{g L}^{-1}$ )                    |         | $Y_{XS}$  | Yield of biomass concentration based on substrate consumption ( $\text{g g}^{-1}$ ) | 0.277  |
| $M_m$    | Maximum specific cell growth rate ( $\text{h}^{-1}$ )                       | 0.001–1 | $Y_{XP}$  | Yield of product formation based on biomass concentration ( $\text{g g}^{-1}$ )     | 1.158  |
| $K_{SX}$ | Substrate inhibition constant for cell growth ( $\text{g L}^{-1}$ )         | 38.850  | $V$   | Bioreactor working volume (L)   | 100    |
| $K_{SS}$ | Substrate inhibition constant for glucose consumption ( $\text{g L}^{-1}$ ) | 44.156  | $X_i$   | Initial concentration of biomass ( $\text{g L}^{-1}$ )                              |        |
| $K_{SP}$ | Substrate inhibition constant for ethanol production ( $\text{g L}^{-1}$ )  | 25.981  | $S_i$   | Initial concentration of substrate (glucose) ( $\text{g L}^{-1}$ )                  |        |
| $S_0$    | Substrate concentration at input stream ( $\text{g L}^{-1}$ )               | 10      | $P_i$   | Initial concentration of product (ethanol) ( $\text{g L}^{-1}$ )                    |        |
| $P_m$    | Ethanol concentration at permeate of bioreactor ( $\text{g L}^{-1}$ )       | 0.01    | $\alpha, \beta, \lambda, \sigma, \kappa, \alpha_1, \lambda_1$ | Grouping parameters   |        |

## REFERENCES

1. ABUALRUB, T, I. SADEK, M. ABUKHALED, Optimal control systems by time-dependent coefficients using cas wavelets, *Journal of Applied Mathematics*, 2009, **2009**, Article ID 636271, 1–10.
2. ABUKHALED, M., Variational iteration method for nonlinear singular two-point boundary value problems arising in human physiology, *Journal of Mathematics*, 2013, **2013**, Article ID 720134, 1–4.
3. ABUKHALED, M., Green's function iterative approach for solving strongly nonlinear oscillators, *Journal of Computational and Nonlinear Dynamics*, 2017, **12**(5), Article ID 051021, 1–5.
4. ARIYAJAROENWONG, P., P. LAOPAIBOON, A. SALAKKAM, P. SRINOPHAKUN, L. LAOPAIBOON, Kinetic models for batch and continuous ethanol fermentation from sweet sorghum juice by yeast immobilized on sweet sorghum stalks, *Journal of the Taiwan Institute of Chemical Engineers*, 2016, **66**, 210–216.
5. AZHAR, S.H.M., R. ABDULLA, S.A. JAMBO, H. MARBAW, G. AZLAN, A.A.M. FAIK, K.F. RODRIGUESC, Yeasts in sustainable bioethanol production: A review, *Biochemistry and Biophysics Reports*, 2017, **10**, 52–61.
6. BAKER, R.W., *Membrane Technology and Applications*, John Wiley & Sons, Ltd., Chischester, 2004.
7. BALAT, M., H. BALAT, Recent trends in global production and utilization of bioethanol fuel, *Applied Energy*, 2009, **86**, 2273–2282.
8. BIROL, G, P. DORUKER, B. KIRDAR, Z.I. ÖNSAN, K. ÜLGEN, Mathematical description of ethanol fermentation by immobilised *Saccharomyces cerevisiae*, *Process Biochemistry* 1998, **33**, 763–771.
9. BRETHAUER, S., C.E. WYMAN, Review: Continuous hydrolysis and fermentation for cellulosic ethanol production, *Bioresource Technology*, 2010, **101**(13), 4862–4874.
10. CAVALHEIRO, A., G. MONTEIRO, J. BRAZ, Solving ethanol production problems with genetically modified yeast strains, *Microbiology*, 2013, **44**(3), 665–671.
11. CHEN, C.L., Y.C. LIU, Solution of two-point boundary-value problems using the differential transformation method, *Journal of Optimization Theory and Applications*, 1998, **99**, 23–35.
12. DE SOUZA, M.M., R.S. GOMES, A. DE BORTOLI, A model for direct ethanol fuel cells considering variations in the concentration of the species, *International Journal of Hydrogen Energy*, 2018, **43**, 13475–13488.
13. DIAZ, C.E., Y.K. SIERRA, J.A. HERNÁNDEZ, Determination of the percentage of ethanol produced by *Saccharomyces cerevisiae* from semi-purified glycerin, IOP Conf. Series: *Journal of Physics: Conf. Series* 2018, **1126**, Article ID 012008, 1–7.
14. ESFAHANIAN, M., A.S. RAD, S. KHOSHHAL, G. NAJAFPOUR, B. ASGHARI, Mathematical modeling of continuous ethanol fermentation in a membrane bioreactor by pervaporation compared to conventional system: Genetic algorithm, *Bioresource Technology*, 2016, **212**, 62–71.
15. GHORI, Q.K., M. AHMED, A.M. SIDDIQUI, Application of homotopy perturbation method to squeezing flow of a Newtonian fluid, *International Journal of Nonlinear Sciences and Numerical Simulation*, 2007, **8**(2), 179–184.
16. GIELEN, D., F. BOSHELL, D. SAYGIN, M.D. BAZILIAN, N. WAGNER, R. GORINI, The role of renewable energy in the global energy transformation, *Energy Strategy Reviews*, 2019, **24**, 38–50.
17. HE, J.H., Homotopy perturbation technique, *Computer Methods in Applied Mechanics and Engineering*, 1999, **178**, 257–262.
18. HE, J.H., Application of homotopy perturbation method to nonlinear wave equations, *Chaos, Solitons and Fractals*, 2005, **26**(3), 695–700.

19. HE, J.H., Variational iteration method-some recent results and new interpretations, *Journal of Computational and Applied Mathematics*, 2007, **207**(1), 3–17.
20. KHURI, S., A. SAYFY, M. ABUKHALED, Spline-based numerical treatments of Bratu-type equations, *Palestine Journal of Mathematics*, 2012, **1**, 63–70.
21. KHURI, S.A., M. ABUKHALED, A semi-analytical solution of amperometric enzymatic reactions based on Green's functions and fixed point iterative schemes, *Journal of Electroanalytical Chemistry*, 2017, **792**, 66–71.
22. KIRTHIGA, M, L. RAJENDRAN, Theoretical treatment of diffusion and kinetics of osmium redoxpolymer mediated glucose oxidase enzyme electrodes: expression of current density for varying potential, *Electrochimica Acta*, 2017, **230**, 84–97.
23. LI, S.J., Y.X. LIU, An improved approach to nonlinear dynamical system identification using PID neural networks, *International Journal of Nonlinear Sciences and Numerical Simulation*, 2006, **7**(2), 177–182.
24. LIMAYEM, A., S.C. RICKE, Lignocellulosic biomass for bioethanol production: Current perspectives, potential issues and future prospects, *Progress in Energy and Combustion Science*, 2012, **38**, 449–467.
25. MARIN, A.R., Y.C. LOPEZ, A.N. GARCIA, J.C.R. HEREDIA, J.C.Z. LORIA, Potential production of ethanol by *Saccharomyces cerevisiae* immobilized and coimmobilized with *Zymomonas mobilis*, in: *Yeast – Industrial Applications*, chap. 11, A. Morata, I. Loira, eds, Intechopen Publisher, UK, 2017, pp. 249–265.
26. MOUSA, M.M., SF. RAGAB, Application of the homotopy perturbation method to linear and nonlinear Schrödinger equations, *Zeitschrift fur Naturforschung – A Journal of Physical Sciences*, 2008, **63**(3), 140–144.
27. OBRIEN, D.J., J.C. CRAIG, Ethanol production in a continuous fermentation/membrane pervaporation system, *Applied Microbiology and Biotechnology*, 1996, **44**(6), 699–704.
28. OZIS, T., A. YILDIRIM, A comparative study of He's homotopy perturbation method for determining frequency-amplitude relation of a nonlinear oscillator with discontinuities, *International Journal of Nonlinear Sciences and Numerical Simulation*, 2007, **8**(2), 243–248.
29. SARAVANAKUMAR, R., P. PIRABAHARAN, M. ABUKHALED, L. RAJENDRAN, Theoretical analysis of voltammetry at a rotating disk electrode in the absence of supporting electrolyte, *Journal of Physical Chemistry B*, 2020, **124**, 443–450.
30. SHOPOVA, E.G., V.N.G. BANCHEVA, BASIC – A genetic algorithm for engineering problems solution, *Computers and Chemical Engineering*, 2006, **30**, 1293–1309.
31. YLITERVO, P., C.J. FRANZÉN, J.M. TAHERZADEH, Continuous ethanol production with a membrane bioreactor at high acetic acid concentrations, *Membranes*, 2014, **4**(3), 372–387.

